Knowledge-Aided Group GLRT for Range Distributed Target Detection in Partially Homogeneous Environment

Yanling Shi(✉)

College of Telecommunications and Information Engineering,
Nanjing University of Post and Telecommunications, Nanjing 210003, China
ylshi@njupt.edu.cn

Abstract. In this paper, we consider the range distributed target detection in partially homogeneous clutter which satisfies a different statistical property in adjacent range cells. The group method wherein adjacent cells with slightly varied statistics are in the same group is presented firstly, which can improve the accuracy of modeling clutter. We assume that all texture of the compound Gaussian clutter satisfies an inverse Gamma distribution but scale and shape parameters in those groups differ from one another. The group generalized likelihood ratio test (G-GLRT) developed here concerns the cells group effects on deducing the GLRT. Considering a knowledge-aided (KA) model that tracking into account the partially homogeneous training samples, we develop a KA-G-GLRT for range-spread target detection and verify the constant false alarm rate (CFAR) with respect to the estimated covariance matrix of speckle. Experimental results are presented to illustrate the performance and effectiveness of the KA-G-GLRT in real clutter data.

Keywords: Group GLRT · Knowledge-aided · Target detection · Partially homogeneous sea clutter · Radar

1 Introduction

In recent years, there have been a large number of investigations on the signal detection problem in sea clutter with unknown covariance matrix (CM) [1–6]. Typically for the low range resolution radar, it is assumed that sea clutter at a range cell under test (CUT), which is also said to be primary data, may have the same statistical property with training samples. These training samples (also called secondary data) obtained from the range cells adjacent to the CUT contain sea clutter only, and are usually used to estimate the CM of sea clutter at the CUT. This scenario is often called homogeneous environment if the adjacent clutter has the same power level and the same CM [7–10]. However, the idealized homogeneous assumption is not suitable for the high radar range resolution, and this environment submits to a partially homogeneous scenario where the adjacent clutter behaves the similar CM structure with a diverse power factor [11, 12]. The higher radar range resolution scenario evolves to the inhomogeneous environment where the adjacent vectors do not share the same CM structure [13]. To mitigate the effects of nonhomogeneity, the authors in [14] advocate

G. Gui and L. Yun (Eds.): ADHIP 2019, LNICST 302, pp. 249–258, 2019.
https://doi.org/10.1007/978-3-030-36405-2_26

a Bayesian approach, and the authors in [15] improve the Bayesian approach to be feasible to the heterogeneous samples, which are more complicated than the inhomogeneous samples. In the heterogeneous scenario, the training data are clustered in groups, each group containing a similar but random CM. Although many authors assumed that the primary data have the same power levels, it is practically not the real case as authors in [16, 17] advocated. The power levels at the CUT were deterministic unknown constants different from each range cell [16], whereas the power levels at the CUT were random variables (RVs) and satisfied the same distribution (see inverse Gamma distribution) but with the significantly different distributed parameters [17]. In the above detectors, the authors only considered the partial homogeneity or the non-homogeneity for the sea clutter at the CUT and assumed the homogeneity for the sea clutter in the secondary data. Sea clutter collected from the sea surface have the same property, no matter they are from the primary data or from the secondary data.

In the paper, we will detect the range distributed target detection in partially homogeneous compound Gaussian (CG) clutter consisting of speckle modulated by texture. The speckle is modeled as a complex Gaussian random vector. The texture is modeled as an unknown deterministic or a RV, mainly satisfies Gamma, inverse Gamma or Pareto distribution [18, 19]. In [17], three types of group generalized likelihood ratio test (G-GLRT) were proposed by using the group strategy according to the variations of scale and shape parameters of texture at the CUT. However, the irrational assumption that secondary data were homogeneous brought a serious detecting performance loss. In [20], the primary and the secondary data were only partially homogeneous to the case in which their covariance matrices are mismatch according to a scaling factor other than one. In [21], Gao et al. modeled the disturbance covariance matrices of the secondary data in MIMO radar as random matrices satisfied the inverse Wishart distribution, and obtained the improved performance. In the paper, we assume secondary data are partially homogeneous and satisfy a knowledge-aided model (such as the inverse Wishart distribution), and develop a KA-G-GLRT for range-spread target detection in partially homogeneous sea clutter. The KA-G-GLRT possess the constant false alarm rate property (CFAR) to the estimated CM of speckle (ECMS). Experimental results are presented to illustrate the performance and effectiveness of the KA-G-GLRT in real clutter data.

The remainder of the paper is organized as follows: next section describes signal model and detection scheme. Section 3 analyzes the CFARness to the ECMS. Experimental results are provided to illustrate the detecting performance of the proposed detector in Sect. 4. Finally, Sect. 5 concludes the paper.

2 Signal Model and Detection Scheme

In the paper, the received echoes $\mathbf{z}_k \in \mathbb{C}^{N\times 1}$, $k = 1, 2, \cdots, K$, are composed of N pulse samples returning from the k-th range cell, where $\mathbb{C}$ being the complex field. Binary hypothesis testing is used to detect the range distributed target in clutter background:

$$\begin{aligned} \mathrm{H}_1 &: \begin{cases} \mathbf{z}_k = \alpha_k \mathbf{p} + \mathbf{c}_{pk} & k = 1, 2, \cdots, K \\ \mathbf{y}_l = \mathbf{c}_{sl} & l = 1, 2, \cdots, L \end{cases} \\ \mathrm{H}_0 &: \begin{cases} \mathbf{z}_k = \mathbf{c}_{pk} & k = 1, 2, \cdots, K \\ \mathbf{y}_l = \mathbf{c}_{sl} & l = 1, 2, \cdots, L \end{cases} \end{aligned}, \tag{1}$$

where, $\mathbf{p} \in \mathbb{C}^{N\times 1}$ is the known nominal steering vector; α_ks are energy distribution ratio of target in different range cells; Primary data $\mathbf{c}_{pk} \in \mathbb{C}^{N\times 1}$ is the additive sea clutter in the k-th range cell; Secondary data $\mathbf{c}_{sl} \in \mathbb{C}^{N\times 1}$ in the l-th range cell has a different CM with the primary data; K and L are the range number of the CUT and that of secondary data, respectively.

With the speckle $\mathbf{g}_k \sim CN(\mathbf{0}, \mathbf{M})$ and random texture τ_k, the primary clutter $\mathbf{c}_{pk}$ is modeled as the CG random process [7–10] with

$$\mathbf{c}_{pk} = \sqrt{\tau_k}\mathbf{g}_k, \quad \tau_k > 0 \tag{2}$$

where $\mathbf{M}$ is known initially, τ_k and $\mathbf{g}_k$ are independent of each other.

Gu et al. claimed that the textures in adjacent cells have different deterministic values [16]. Furthermore, Shi found that the textures behaved statistically different in adjacent cells, i.e. the parameters of PDF vary [17]. Referring to the group strategy [17] in partially homogeneous clutter environments, we firstly divide the K range cells into G groups, and h_g, $g = 1, 2, \cdots, G$, is the cell number in each group, $\sum_{g=1}^{G} h_g = K$.

It has been verified in [18] that the CG model with inverse Gamma texture is suitable for modeling clutter data. Therefore, we assume that the textures in all G groups satisfy an inverse Gamma distribution but scale parameters β_g and shape parameters η_g in those groups differ from one another. That reads

$$\begin{aligned} &f_{IG}(\tau_k; \beta_g, \eta_g) = \frac{\beta_g^{\eta_g}}{\Gamma(\eta_g)} \frac{1}{\tau_k^{\eta_g+1}} \exp\left(-\frac{\beta_g}{\tau_k}\right), g = 1, 2, \cdots, G, \\ &H_g + 1 \le k \le H_g + h_g, \quad \tau_k > 0 \end{aligned} \tag{3}$$

where

$$H_g = \begin{cases} 0, & g = 1 \\ \sum_{i=1}^{g-1} h_i, & g = 2, 3, \cdots, G \end{cases}, \quad \beta_g > 0, \quad \eta_g > 0 \tag{4}$$

The group partially homogeneous texture satisfies $f_{IG}(\tau_k; \beta_{g_1}, \eta_{g_1}) \neq f_{IG}(\tau_k; \beta_{g_2}, \eta_{g_2})$, if $g_1 \neq g_2$ and $g_1, g_2 = 1, 2, \cdots, G$. Define $\boldsymbol{\beta} = [\beta_1, \beta_2, \cdots, \beta_G]$, $\boldsymbol{\eta} = [\eta_1, \eta_2, \cdots, \eta_G]$ and $\mathbf{h} = [h_1, h_2, \cdots, h_G]$.

With $\mathbf{g}_k \sim CN(\mathbf{0}, \mathbf{M})$, the joint PDFs of $\mathbf{z}_1, \cdots, \mathbf{z}_K$ are

$$f_i(\mathbf{z}_1,\cdots,\mathbf{z}_K)=\int_0^{\infty} f_i(\mathbf{z}_1,\cdots,\mathbf{z}_K|\tau_k)f_{IG}(\tau_k;\beta_g,\eta_g)d\tau_k$$
$$=\prod_{g=1}^{G}\left[\frac{\beta_g^{\eta_g}\Gamma(N+\eta_g)}{\Gamma(\eta_g)|\mathbf{M}|}\right]^{h_g}\prod_{k=H_g+1}^{H_g+h_g}\left((\mathbf{z}_k-i\alpha_k\mathbf{p})^{\mathrm{H}}\mathbf{M}^{-1}(\mathbf{z}_k-i\alpha_k\mathbf{p})+\beta_g\right)^{-(N+\eta_g)}, \tag{5}$$

where $i=0$ and $i=1$ correspond to H_0 and H_1, respectively. With the estimated parameters α_k, β_g and η_g by the maximum likelihood estimator and the method of moments, respectively, the G-GLRT is given by [17],

$$\sum_{g=1}^{G}\sum_{k=H_g+1}^{H_g+h_g}-(N+\eta_g)\ln\left[1-\frac{\left|\mathbf{p}^{\mathrm{H}}\mathbf{M}^{-1}\mathbf{z}_k\right|^2}{\left(\mathbf{z}_k^{\mathrm{H}}\mathbf{M}^{-1}\mathbf{z}_k+\beta_g\right)\left(\mathbf{p}^{\mathrm{H}}\mathbf{M}^{-1}\mathbf{p}\right)}\right]\underset{\mathrm{H}_0}{\overset{\mathrm{H}_1}{\gtrless}}\ln\xi\,. \tag{6}$$

β_g are different in G groups, so are η_gs, the scenario is suitable for the group partially homogeneous clutter environment. When $\beta_{g_1}=\beta_{g_2}$ and $\eta_{g_1}=\eta_{g_2}$, with $g_1\neq g_2$ and $g_1,g_2=1,2,\cdots,G$, in this case, the G-GLRT reduces to the GLRT due to the homogeneous scenario [18].

Notice that, the known CMS $\mathbf{M}$ is not suitable in the partially homogeneous environment, we can establish the relationship for the CMS between in primary data and in secondary data. Firstly, we model $\mathbf{M}$ as a complex inverse Wishart random matrix [21],

$$\mathbf{M}\sim CW_N^{-1}(v,\lambda(v-N)\bar{\mathbf{M}}) \tag{7}$$

where v denotes the degrees of freedom of the inverse Wishart distribution, $(v-N)\bar{\mathbf{M}}$ denotes the prior CM structure, and λ denotes the power level of speckle. The PDF of $\mathbf{M}$ is given by

$$f(\mathbf{M})=\frac{|\lambda(v-N)\bar{\mathbf{M}}|^v}{\bar{\Gamma}_N(v)|\mathbf{M}|^{v+N}}etr[-(v-N)\lambda\mathbf{M}^{-1}\bar{\mathbf{M}}] \tag{8}$$

where $\bar{\Gamma}_N(v)=\pi^{N(N-1)/2}\prod_{n=1}^{N}\Gamma(v-n+1)$.

Then, we consider the maximum a posteriori (MAP) estimate of $\mathbf{M}$ by using the secondary data $\mathbf{y}_l$, $l=1,\cdots,L$,

$$\begin{aligned}\hat{\mathbf{M}}&=\arg\max_{\mathbf{M}}f(\mathbf{y}_1,\cdots,\mathbf{y}_L|\mathbf{M})f(\mathbf{M})\\&\propto\frac{\lambda^{Nv}}{|\mathbf{M}|^{v+N+L}}etr\{-\mathbf{M}^{-1}[\mathbf{S}+(v-N)\lambda\bar{\mathbf{M}}]\}\end{aligned} \tag{9}$$

where $\mathbf{S}=\sum_{L=1}^{L}\mathbf{y}_l\mathbf{y}_l^{\mathrm{H}}$. It follows from (9) that

$$\max_{\mathbf{M}}(v+N+L)\log(|\mathbf{M}^{-1}|)-tr\{\mathbf{M}^{-1}[\mathbf{S}+(v-N)\lambda\bar{\mathbf{M}}]\} \tag{10}$$

Referring to the conclusion in [21], we have

$$\hat{\mathbf{M}}=\frac{\mathbf{S}+(v-N)\lambda\bar{\mathbf{M}}}{v+N+L} \tag{11}$$

Substituting $\hat{\mathbf{M}}$ into (6), we obtain the KA-G-GLRT as

$$\sum_{g=1}^{G}\sum_{k=H_g+1}^{H_g+h_g}-(N+\eta_g)\ln\left[1-\frac{\left|\mathbf{p}^{\mathrm{H}}\hat{\mathbf{M}}^{-1}\mathbf{z}_k\right|^2}{\left(\mathbf{z}_k^{\mathrm{H}}\hat{\mathbf{M}}^{-1}\mathbf{z}_k+\beta_g\right)\left(\mathbf{p}^{\mathrm{H}}\hat{\mathbf{M}}^{-1}\mathbf{p}\right)}\right]\underset{\mathrm{H}_0}{\overset{\mathrm{H}_1}{\gtrless}}\ln\xi\,. \tag{12}$$

3 CFAR Property of the KA-G-GLRT

In this section, we focus on the CFAR property of the KA-G-GLRT. It has been testified in [17] that the G-GLRT has the CFAR property to β_g and $\mathbf{M}$. Here, we prove the KA-G-GLRT also has the CFARness to $\hat{\mathbf{M}}$.

Since the left-hand side of the KA-G-GLRT contains a RV $\hat{w}_k$,

$$\hat{w}_k=\frac{\left|\mathbf{p}^{\mathrm{H}}\hat{\mathbf{M}}^{-1}\mathbf{z}_k\right|^2}{\left(\mathbf{z}_k^{\mathrm{H}}\hat{\mathbf{M}}^{-1}\mathbf{z}_k+\beta_g\right)\left(\mathbf{p}^{\mathrm{H}}\hat{\mathbf{M}}^{-1}\mathbf{p}\right)} \tag{13}$$

the CFAR property to the $\hat{\mathbf{M}}$ of the KA-G-GLRT lies in whether the RV $\hat{w}_k$ is independent of the CMS, which will be shown as follows.

Let

$$\boldsymbol{\upsilon}_k=\mathbf{M}^{-1/2}\mathbf{g}_k,\boldsymbol{\mu}_l=\mathbf{M}^{-1/2}\mathbf{g}_l,l=1,\cdots,L,\mathbf{p}_0=\mathbf{M}^{-1/2}\mathbf{p} \tag{14}$$

Then, $\boldsymbol{\upsilon}_k\sim CN(\mathbf{0},\mathbf{I}_N)$, $\boldsymbol{\mu}_l\sim CN(\mathbf{0},\mathbf{I}_N),l=1,\cdots,L$. Under the H_0 hypothesis,

$$\mathbf{z}_k^{\mathrm{H}}\hat{\mathbf{M}}^{-1}\mathbf{z}_k=\tau_k\mathbf{g}_k^{\mathrm{H}}\hat{\mathbf{M}}^{-1}\mathbf{g}_k=\tau_k\boldsymbol{\upsilon}_k^{\mathrm{H}}\left(\mathbf{M}^{-1/2}\hat{\mathbf{M}}\mathbf{M}^{-1/2}\right)^{-1}\boldsymbol{\upsilon}_k=\tau_k\boldsymbol{\upsilon}_k^{\mathrm{H}}\mathbf{W}^{-1}\boldsymbol{\upsilon}_k \tag{15}$$

where

$$\begin{aligned}\mathbf{W}&=\mathbf{M}^{-1/2}\hat{\mathbf{M}}\mathbf{M}^{-1/2}=\frac{1}{v+N+L}\mathbf{M}^{-1/2}\mathbf{S}\mathbf{M}^{-1/2}+\frac{(v-N)\lambda}{v+N+L}\mathbf{M}^{-1/2}\bar{\mathbf{M}}\mathbf{M}^{-1/2}\\&=\frac{1}{v+N+L}\sum\nolimits_{L=1}^{L}\tau_l\boldsymbol{\mu}_l\boldsymbol{\mu}_l^{\mathrm{H}}+\frac{(v-N)\lambda}{v+N+L}\mathbf{M}^{-1/2}\bar{\mathbf{M}}\mathbf{M}^{-1/2}\end{aligned} \tag{16}$$

Set $\mathbf{X}\mathbf{X}^{\mathrm{H}} = \sum_{L=1}^{L} \boldsymbol{\mu}_l \boldsymbol{\mu}_l^{\mathrm{H}}$, here, $\sum_{L=1}^{L} \tau_l \boldsymbol{\mu}_l \boldsymbol{\mu}_l^{\mathrm{H}} = \mathbf{X}\boldsymbol{\Lambda}\mathbf{X}^{\mathrm{H}}$, and $\boldsymbol{\Lambda} = diag(\tau_l)$. Due to $\boldsymbol{\mu}_l \sim CN(\mathbf{0}, \mathbf{I}_N)$, we have $\boldsymbol{\Lambda}^{-1/2}\boldsymbol{\mu}_l \sim CN(\mathbf{0}, \boldsymbol{\Lambda})$, and $\mathbf{X}\boldsymbol{\Lambda}\mathbf{X}^{\mathrm{H}}$ satisfies the complex Wishart distribution with $\mathbf{X}\boldsymbol{\Lambda}\mathbf{X}^{\mathrm{H}} \sim CW_N(\mathbf{I}_N, \boldsymbol{\Lambda})$ for the IID random vectors $\boldsymbol{\mu}_l$. $\mathbf{M}^{-1/2}\bar{\mathbf{M}}\mathbf{M}^{-1/2}$ is a constant with the known $\bar{\mathbf{M}}$. Hence, random matrix $\mathbf{W}$ follows the complex Wishart distribution. Thus, $\mathbf{z}_k^{\mathrm{H}}\hat{\mathbf{M}}^{-1}\mathbf{z}_k$ under the H_0 hypothesis is independent of the CMS $\hat{\mathbf{M}}$.

Further, rotate the vector $\mathbf{p}_0$ into the first coordinate vector, and setting $\tilde{\boldsymbol{\upsilon}} = \mathbf{U}^{\mathrm{H}}\boldsymbol{\upsilon} \sim CN(\mathbf{0}, \mathbf{I})$, we have $\left|\mathbf{p}^{\mathrm{H}}\hat{\mathbf{M}}^{-1}\mathbf{z}_k\right|^2 / \left(\mathbf{p}^{\mathrm{H}}\hat{\mathbf{M}}^{-1}\mathbf{p}\right)$

$$\frac{\left|\mathbf{p}^{\mathrm{H}}\hat{\mathbf{M}}^{-1}\mathbf{z}_k\right|^2}{\mathbf{p}^{\mathrm{H}}\hat{\mathbf{M}}^{-1}\mathbf{p}} = \frac{\left|\mathbf{p}_0^{\mathrm{H}}\mathbf{W}^{-1}\boldsymbol{\upsilon}_k\right|^2}{\mathbf{p}_0^{\mathrm{H}}\mathbf{W}^{-1}\mathbf{p}_0} = \frac{\left|\mathbf{e}_1^{\mathrm{H}}\tilde{\mathbf{W}}^{-1}\tilde{\boldsymbol{\upsilon}}_k\right|^2}{\mathbf{e}_1^{\mathrm{H}}\tilde{\mathbf{W}}^{-1}\mathbf{e}_1} \tag{17}$$

where

$$\begin{aligned} &\tilde{\mathbf{W}} = \mathbf{U}^{\mathrm{H}}\mathbf{W}\mathbf{U} = \frac{1}{v+N+L}\mathbf{U}^{\mathrm{H}}\sum_{l=1}^{L}\tau_l\boldsymbol{\mu}_l\boldsymbol{\mu}_l^{\mathrm{H}}\mathbf{U} + \frac{(v-N)\lambda}{v+N+L}\mathbf{U}^{\mathrm{H}}\mathbf{M}^{-1/2}\bar{\mathbf{M}}\mathbf{M}^{-1/2}\mathbf{U}, \\ &\mathbf{e}_1 = \mathbf{U}^{\mathrm{H}}\mathbf{p}_0, \quad \mathbf{e}_1 = [1\,0\,0\,\cdots\,0]^{\mathrm{T}} \end{aligned} \tag{18}$$

and $\mathbf{U}$ is a unitary matrix.

Table 1. The energy distribution ratio α_k of the range distributed target

Cell index	1	2	3	4	5	6	7	8	9	10	11	12
Model1	1/12	1/12	1/12	1/12	1/12	1/12	1/12	1/12	1/12	1/12	1/12	1/12
Model2	1/3	0	1/3	0	0	0	0	0	0	0	0	0
Model3	1/3	0	1/3	0	1/3	0	0	0	0	0	0	0
Model4	1/4	1/4	1/4	1/4	0	0	0	0	0	0	0	0

Similarly, the reasons that the random matrix $\mathbf{U}^{\mathrm{H}}\sum_{l=1}^{L}\tau_l\boldsymbol{\mu}_l\boldsymbol{\mu}_l^{\mathrm{H}}\mathbf{U} \sim CW_N(\mathbf{I}, \mathbf{U}^{\mathrm{H}}\boldsymbol{\Lambda}\mathbf{U})$ and $\mathbf{U}^{\mathrm{H}}\mathbf{M}^{-1/2}\bar{\mathbf{M}}\mathbf{M}^{-1/2}\mathbf{U}$ is a constant result in the random matrix $\tilde{\mathbf{W}}$ following the complex Wishart distribution.

Finally, the RV $\hat{w}_k$ can be rewritten as

$$\hat{w}_k = \frac{\left|\mathbf{e}_1^{\mathrm{H}}\tilde{\mathbf{W}}^{-1}\tilde{\boldsymbol{\upsilon}}_k\right|^2}{\left(\tau_k\boldsymbol{\upsilon}_k^{\mathrm{H}}\mathbf{W}^{-1}\boldsymbol{\upsilon}_k + \beta_g\right)\left(\mathbf{e}_1^{\mathrm{H}}\tilde{\mathbf{W}}^{-1}\mathbf{e}_1\right)} \tag{19}$$

Obviously, $\hat{w}_k$ is independent of the CMS $\hat{\mathbf{M}}$. Therefore, the KA-G-GLRT has the CFAR property to $\hat{\mathbf{M}}$.

In the following section, the performance of KA-G-GLRT will be evaluated.

4 Experimental Results and Performance Evaluation

We will evaluate the performance of the KA-G-GLRT and the compared detectors (1S-G-GLRT [17], GCC-GLRT [16], OS-GLRT [5], and NSDD-GLRT [4]) by Fynmeet radar data. The point that we wish to make that although the 1S-G-GLRT and the GCC-GLRT applied the group method, the former assumed that τ_ks were RVs in different range cells and the secondary data were homogeneous, and the later assumed that τ_ks were the unknown and different constants in all groups, whose values can be estimated by the likelihood estimator from the received sea echoes. In contrast, in our KA-G-GLRT, τ_k satisfies an inverse Gamma distribution with different parameters in G groups and the secondary data are partially homogeneous with an inverse Wishart distribution, which is a better approximation of the real complicated scenario than that in the 1S-G-GLRT and in the GCC-GLRT. The range distributed target is the multiple dominant scattering (MDS) model [16]. Set $K = 12$, the energy distribution ratio α_k of the target in each range cell is shown in Table 1.

The signal to clutter ratio is

$$SCR = \frac{1}{P_c}\sum\nolimits_{k=1}^{K} |A\alpha_k|^2, \tag{20}$$

where A is the amplitude of detecting target, and P_c is the power of $\mathbf{c}_{pk}$. $\bar{\mathbf{M}}$ is given by $\rho^{|i-j|}$ with a one-lag correlation coefficient ρ.

The analyzed data are TFA10-006 recorded by the Fynmeet radar in 2006 [22]. Figure 1 shows the detection performance of five detectors versus SCR with the parameters $L = 48$, $N = 4$, $K = 12$, $G = 3$, $\rho = 0$, $v = 24$, $\lambda = 2$, $\boldsymbol{\beta} = [0.133, 0.112, 0.604]$, $\boldsymbol{\eta} = [3.491, 2.260, 6.695]$, $\mathbf{h} = [3, 3, 6]$ and $P_f = 10^{-3}$. The reason of group may refer to [17]. The KA-G-GLRT behaves best for all five models, such as in model 4 (see Fig. 1(d)), the 1S-G-GLRT is below the KA-G- GLRT by approximately 1 dB, the OS-GLRT present about 2 dB worse, and the GCC-GLRT and NSDD-GLRT present about 3 dB worst. The NSDD-GLRT and the OS-GLRT are overcome by the KA-G-GLRT since the assumed homogeneous clutter in these two detectors deviates from the real clutter that is partially homogeneous. The simplified assumption that texture is an unknown constant leads to the worse behaviors of the GCC-GLRT than the KA-G-GLRT wherein the random texture, much more coinciding with the real environment, is used. Meanwhile, the KA speckle helps to promote the detection performance of the KA-G-GLRT compared to the 1S-G-GLRT. We can therefore draw a conclusion that the KA-G-GLRT behaves best in all four target models, and it has a more extensive applicability.

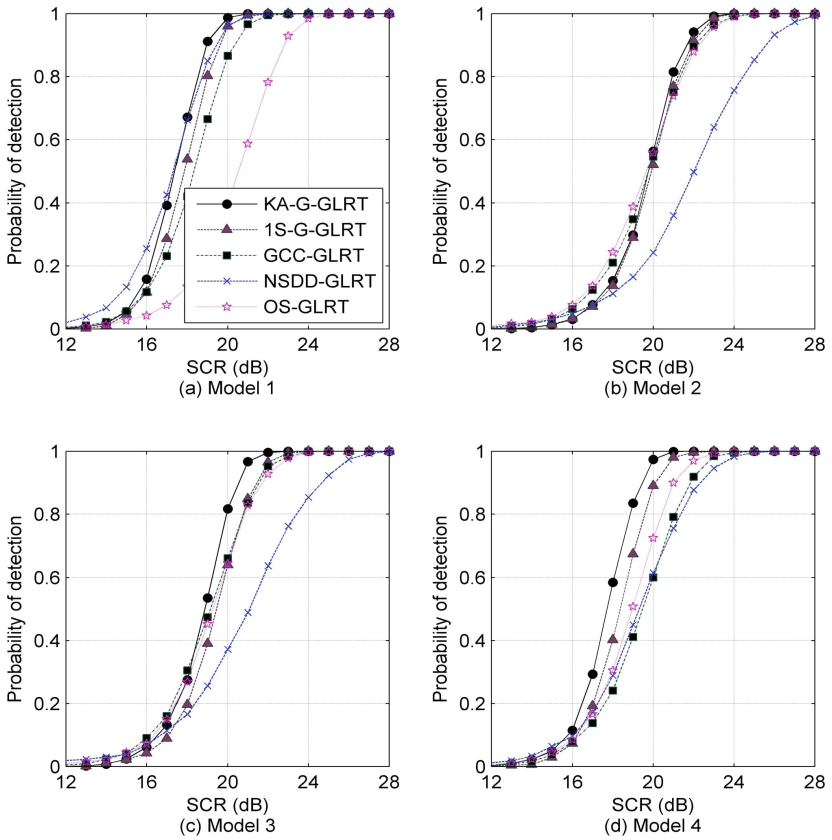

Fig. 1. Probability of detection versus SCR for the real data. (a) Model 1; (b) Model 2; (c) Model 3; (d) Model 4.

5 Conclusion

In this paper, we have dealt with the range distributed target detection in the grouped partially homogeneous clutter environment. CG clutter has been composed of inverse Gamma partially homogeneous texture and Gaussian speckle. A stochastic KA model with complex inverse Wishart distribution was introduced, where the CMS exhibits partially homogeneity. The KA-G-GLRT detector has been proposed in the paper. Having the range cells grouped guarantees that texture satisfies an inverse Gamma distribution but scale and shape parameters in those groups differ from one another. The KA-G-GLRT is CFAR with respect to the ECM. The experimental performance shows that, for four different MDS target models, the KA-G-GLRT outperforms the 1S-G-GLRT, GCC-GLRT, OS-GLRT and NSDD-GLRT, and has a more extensive applicability in the real sea clutter. The validity of the KA-G-GLRT in partially homogeneous clutter environment has been verified at length.

Acknowledgement. The work was supported by the National Natural Science Funds (61201325) and NUPTSF (NY218045).

References

1. Ernesto, C., De Antonio, M., Giuseppe, R.: GLRT-based adaptive detection algorithms for range-spread targets. IEEE Trans. Signal Process. **49**(7), 1336–1348 (2001)
2. Karl, G.: Detection of a spatially distributed target in white noise. IEEE Signal Process. Lett. **4**(7), 198–200 (1997)
3. Karl, G., Steiner, M.J.: Adaptive detection of range distributed targets. IEEE Trans. Signal Process. **47**(7), 1844–1851 (1999)
4. Karl, G.: Spatially distributed target detection in non-Gaussian clutter. IEEE Trans. Aerosp. Electron. Syst. **35**(3), 926–934 (1999)
5. He, Y., Jian, T., Su, F., Qu, C.W., Gu, X.: Novel range-spread target detectors in non-Gaussian clutter. IEEE Trans. Aerosp. Electron. Syst. **46**(3), 1312–1328 (2010)
6. Domenico, C., De Antonio, M., Danilo, O.: On the statistical invariance for adaptive radar detection in partially homogeneous disturbance plus structured interference. IEEE Trans. Signal Process. **65**(5), 1222–1234 (2017)
7. Xu, S.W., Shui, P.l., Yan, X.Y., Cao, Y.H.: Combined adaptive normalized matched filter detection of moving target in sea clutter. Circ. Syst. Signal Process. **36**(6), 2360–2383 (2017)
8. Francesco, B., Olivier, B., Giuseppe, R.: Adaptive detection of distributed targets in compound-Gaussian noise without secondary data: a Bayesian approach. IEEE Trans. Signal Process. **59**(12), 5698–5708 (2011)
9. Shi, Y.L., Shui, P.L.: Target detection in high-resolution sea clutter via block-adaptive clutter suppression. IET Radar Sonar Navig. **5**(1), 48–57 (2011)
10. Shui, P.L., Shi, Y.L.: Subband ANMF detection of moving targets in sea clutter. IEEE Trans. Aerosp. Electron. Syst. **48**(4), 3578–3593 (2012)
11. Shi, B., Hao, C.P., Hou, C.H., Ma, X.C., Peng, C.Y.: Parametric Rao test for multichannel adaptive detection of range-spread target in partially homogeneous environments. Signal Process. **108**, 421–429 (2015)
12. Hao, C.P., Danilo, O., Ma, X.C., Hou, C.H.: Persymmetric Rao and Wald tests for partially homogeneous environment. IEEE Signal Process. Lett. **19**(9), 587–590 (2012)
13. Muralidhar, R.: Statistical analysis of the nonhomogeneity detector for non-Gaussian interference backgrounds. IEEE Trans. Signal Process. **53**(6), 2101–2111 (2005)
14. Stephanie, B., Olivier, B., Jean, Y.T.: A Bayesian approach to adaptive detection in nonhomogeneous environments. IEEE Trans. Signal Process. **56**(1), 205–217 (2008)
15. Olivier, B., Stephanie, B., Jean, Y.T.: Covariance matrix estimation with heterogeneous samples. IEEE Trans. Signal Process. **56**(3), 909–920 (2008)
16. Gu, X.F., Jian, T., He, Y., Su, F., Tang, X.M.: GLRT detector of range spread target in local homogeneous background and its performance analysis. Acta Electron. Sin. **41**(12), 2367–2373 (2013)
17. Shi, Y.L.: Three GLRT detectors for range distributed target in grouped partially homogeneous radar environment. Signal Process. **135**(6), 121–131 (2017)
18. Shang, X., Song, H.: Radar detection based on compound-Gaussian model with inverse gamma texture. IET Radar Sonar Navig. **5**(3), 315–321 (2011)
19. Graham, V.W.: Development of an improved minimum order statistic detection process for Pareto distributed clutter. IET Radar Sonar Navig. **9**(1), 19–30 (2015)

20. Olivier, B., Louis, L.S., Shawn, K.: Adaptive detection of a signal known only to lie on a line in a known subspace, when primary and secondary data are partially homogeneous. IEEE Trans. Signal Process. **54**(12), 4698–4705 (2006)
21. Gao, Y.C., Li, H.B., Braham, H.: Knowledge-aided range-spread target detection for distributed MIMO radar in nonhomogeneous environments. IEEE Trans. Signal Process. **65** (3), 617–627 (2017)
22. Herselman, P.L., Baker, C.J., de Wind, H.J.: An analysis of X-band calibrated sea clutter and small boat reflectivity at medium-to-low grazing angles. Int. J. Navig. Obs. **2008**, 14 pages (2008)